

Size effects in the resistivity of epitaxial films of silver*

A. Berman[†] and H. J. Juretschke

Polytechnic Institute of New York, Brooklyn, New York 11201

(Received 30 October 1974)

The resistivity of epitaxial silver films on mica in vacuum is studied as a function of temperature, thickness, and surface conditions. All samples share a common mica-silver interface. Surface roughness of the other surface is controlled by low-temperature evaporation of very thin silver overlays that anneal below room temperature. The strongly interdependent data are interpreted by rigorous fits to various models of size effects. The fits yield reasonable parameter values, some of which imply temperature-dependent surface scattering. It is shown that resistivity data alone do not suffice to distinguish between different theories of size effects or to identify the detailed aspects of surface scattering.

I. INTRODUCTION

Electrical size effects, indicative of the relative contributions to the resistivity of volume and surface scattering by current carriers, become important when the ratio $K=t/\lambda$ (t is the smallest sample dimension, λ is the bulk mean free path) is of order unity or less.¹ In thin films, where t is the film thickness, this range of interest of K is usually spanned either by studying the resistance of samples of different thicknesses at a given temperature or by examining a single sample over a sufficiently large range of temperatures.² The first approach requires that the various samples, prepared independently by the same technique, have common volume and surface properties and differ only in t . In the second, the temperature dependence of bulk scattering must be known and one has to allow for a possible temperature variation of surface scattering.

Considering the practical difficulties in preparing many samples with identical properties, and in knowing the bulk properties over a large range of temperatures of an infinitely thick sample prepared in the same manner, a meaningful interpretation of experimental data obtained by either approach is often hard to justify. While it is nearly always possible to fit a limited set of data to a particular theory, the fit is far from unique in terms of the three or more parameters of any such theory. Furthermore, the interpretation is sensitive to the specific combinations of experimental data chosen for the fit. For example, a fit obtained for $\rho(t)$ and $\alpha(t)=(1/\rho)d\rho/dT$, commonly applied in the literature of size effects, usually does not reproduce the experimentally found temperature variation $d\rho/dT$, taken by itself.

In view of these difficulties, a rigorous interpretation of size effects must meet stringent conditions. Preferably, it requires an overdeter-

mined set of experimental data covering a good range of all variables of a given theory. This input must lead to over-all and internally consistent agreement of all data with a well-defined, reasonable set of the theoretical parameters. It presupposes a group of samples tied to each other by common or well-reproducible volume properties and common or independently controllable surface conditions.

We have completed such a study on a group of epitaxial films of silver on mica.³ These films were prepared primarily to measure the metallic field effect,⁴ but since knowledge of their size-effect behavior is a prerequisite for analyzing other transport phenomena such as the field effect, both types of measurement were carried out concurrently. To obtain strongly interdependent data on a group of films with well-characterized properties we adopted the following experimental design:

1—A thin film of 300–400 Å is epitaxially grown by vapor deposition on mica, and annealed to high crystallinity.

2—The resistance of the film is measured in vacuum for at least one full temperature cycle between the film annealing temperature T_{af} and that of liquid nitrogen T_N .

3—Without breaking vacuum, a 15–30-Å layer is deposited on the film surface at T_N to produce a slightly thicker film of higher resistance. The new resistance is measured for at least one temperature cycle in the range of temperatures $T_N \leq T < T_{as}$ in which this surface layer remains unannealed.

4—The resistance is then measured as the film temperature is raised to the surface annealing temperature T_{as} and above, and a complete measurement cycle of step 2 is carried out once the surface layer is fully annealed.

5—Without breaking vacuum, a new layer of the same order of thickness as the original film is de-

posited on the sample, and the new sample is annealed and measured, repeating steps 1 and 2. This is followed by steps 3 and 4.

6—The procedure of step 5 is repeated once more, for a third layer, to give a film of total thickness of about 1000 Å. Figure 1 summarizes this sequence of steps in terms of the actual numbers applying to the three nominal film thicknesses whose properties are reported and analyzed here.

The experimental conditions and procedures that were especially observed for obtaining reproducible results are described in Sec. II. Section III is a summary of the results of the measurements and their implications. Interpretation of the data in terms of detailed models of size effects is given in Secs. IV and V.

II. EXPERIMENTAL SUMMARY

A. Sample preparation

All samples were deposited on commercially precut and precleaved ruby muscovite mica about 0.005 cm thick. (Freshly cleaved mica yielded films with less-ordered crystal structure.) The mica was cleaned by washing in a wetting agent, hot distilled water, and then distilled acetone.

To avoid having to break the vacuum during the course of the experiment, the electrical contacts for four-probe measurement of resistance were affixed to the mica substrate before the first evaporation. These contacts consisted of evaporated silver connected to thin silver wires by water-based epoxy bonded to both the bare mica and the silver. The contacts had very low resistance and did not influence the measurements. They performed reliably for the many temperature cycles and successive evaporations of the experiment.

The basic layers of silver, each of about 300 Å, were evaporated at a rate of approximately 100 Å/sec, at a throw of 25 cm, from pure silver wound around molybdenum filaments. At the on-

set of evaporation the chamber pressure was about 10^{-6} Torr. The substrate temperature was held around 175 to 200 °C, depending on the total film thickness. All films were annealed at 200 to 225 °C for at least an hour. The thin "skins" were evaporated very slowly at lower than 100 °K to thicknesses of between 15 and 30 Å.

B. Sample characterization

After the conclusion of the experiment, the thicknesses of the various layers were measured by multiple-beam interferometry on a separate plate next to the sample which recorded a step for each successive layer. Thicknesses so obtained agreed very closely with those deduced from the fringes of x-ray diffraction peaks of the same film. The thickness of the skins was determined primarily by a quartz-crystal thickness monitor.

The crystal structure and perfection of the sample were examined by x-ray Laue transmission with Cu radiation, which gave strong diffraction from the (111) planes even for the thinnest films.^{3,5} Such Laue pictures yield six heavy evenly placed spots at the radius corresponding to the (111) plane spacing in silver. The presence of six spots rather than three is associated with "double positioning" caused by twinning, as pointed out by Pashley.⁶ The same exposure established a definite orientation of the silver with respect to the mica.

Low-energy electron diffraction of the annealed surfaces gave very sharp spots indicating a highly ordered surface. Transmission electron-microscope pictures showed that the thinnest single-crystal film examined, about 300 Å thick, was highly continuous and that any holes in the films covered less than 1% of the area of the film.

The vacuum during the electrical measurements was around 10^{-7} Torr, leading to some residual gas adsorption on the free film surfaces. How-

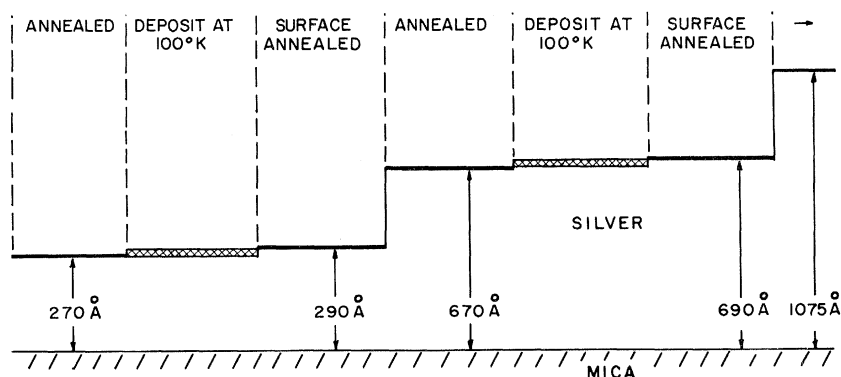


FIG. 1. Sequence of film depositions and measurements for the three-layer experiment analyzed in the text.

ever, our results indicate that the free film surfaces of well-annealed epitaxial films react only very weakly with any ambient atmosphere. Thus, when exposed to air, they show much less tarnishing than surfaces of polycrystalline films. Furthermore, during the experiments at 10^{-7} Torr we did not observe any electrical effects of the boundaries between successive layers of silver. Hence, we believe that in our samples any adsorbed film remained very thin and was removed from the surface upon deposition and annealing of additional material.

C. Design of measurements

The experiment required cycling the sample, in vacuum, between 100 and 600 °K, while making continuous electrical measurements. With the sample temperature changing at a rate of about 30 °C/h, thermal quasiequilibrium was maintained by enclosing the sample in hardware arranged as a vacuum Dewar. After evaporation the Dewar was closed by a shutter and was entirely enclosed in a stainless-steel outer shell.

Thermal inertia for temperature smoothing was obtained by having the sample sit on a thick copper base which could be heated electrically or cooled by liquid nitrogen. Temperature gradients in the area of the sample were less than 2 °K throughout most of the thermal cycle. Below 125 °K the system moved very slowly and a residual gradient of 6–10 °K could develop from copper base to sample because of the poor conducting properties of the mica.

The temperature was automatically cycled by a programmed thermal control unit and electrical measurements of current and voltage were recorded nearly continuously, along with the sample temperature. In runs over two or more thermal cycles the reproducibility of the film resistance was typically (1–2)%.

For a single sample the global estimate of the uncertainty in the absolute value of the resistivity at room temperature is 8% for a 300-Å film and 5% for 1000-Å film. At the lowest temperatures a somewhat greater range cannot be excluded because of the uncertainty in temperature of the sample. From sample to sample, however, the electrical properties reported here have been reproducible and consistent to well within these estimates.

III. RESULTS

The results of the measurements fall into two categories. First there are qualitative conclusions that apply to all observations. Second, there are the detailed quantitative features of the sys-

tematic program outlined in the Introduction.

Two annealing temperatures were found. One, around 400 °K, is the temperature T_{af} at which the film assumes a stable single-crystalline structure. The other, around 250 °K, describes the temperature T_{as} in whose neighborhood a skin of about 10–30 Å deposited at low temperatures anneals and presumably becomes an ordered part of the underlying previously annealed film.

Once the film is annealed, its resistance R is a reproducible and reversible function of temperature (for $T < T_{af}$), and is unchanged upon repeated cycling of the temperature in vacuum. For the annealed film with a rough skin, the same reproducibility in R applies in the range $T_N < T < T_{as}$. If T_{as} is exceeded, however, R drops irreversibly to a new curve over a range of about 50° and then again follows a reversible path between T_N and T_{af} characteristic of a somewhat thicker fully annealed film.

The resistance R was recorded in intervals of about 1 °K, and a typical complete plot of such data is shown in Fig. 2. Although there are small local fluctuations, the over-all result gives a linear temperature dependence of R over the whole temperature range. This linearity applies to all of the data, as long as they were on the reversible part of the experimental cycle, and such linear representation will be used below in presenting the results.

Figure 3 details the effect of depositing a thin overlay on an annealed film. Curve (2) shows R of the original film. Curve (3) gives the R of the now somewhat thicker film, but having a rough surface, and it includes the transition to the annealed state. (The temperature was raised at the rate of 0.5 °K/min; it is not certain to what extent the behavior in this transition region depends on this rate.) Finally, curve (4) shows the resistance of the film after the overlay is fully annealed. These data confirm Lucas's observations⁷ of the effect on R of a very thin rough overlay, and extend them to include the variation with temperature of this effect in silver. Clearly, the effect will not be observed if the skin is laid down around room temperature.⁸ It is to be noted that a rougher surface leads not only to a much higher film resistance, but also to a significantly smaller temperature variation of this resistance. After full anneal the final film has at all temperatures a slightly lower resistance than at the beginning, as to be expected since its thickness has increased slightly.

Figure 4 summarizes the results of a full sequence of deposits and temperature cycles as outlined in Sec. I. At each thickness it shows the resistivity ρ for the film before and after annealing

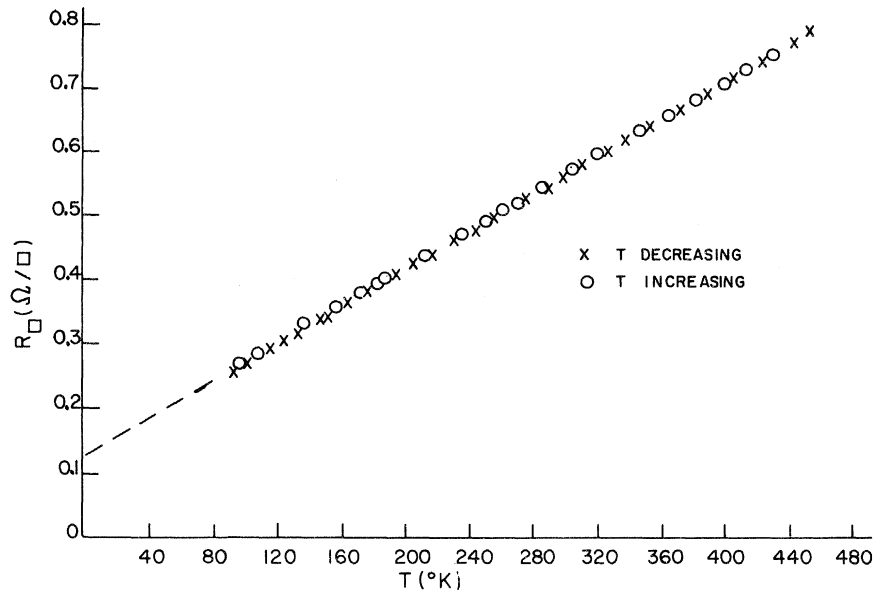


FIG. 2. Experimentally recorded film resistance vs temperature. $t \sim 350 \text{ \AA}$. R_{\square} is the resistance per square of the film.

of the overlay. The corresponding curve for bulk silver is also included.⁹ The most obvious feature of these curves is the thickness variation of the film resistivity. As expected, and well known, the resistivity decreases with increasing thickness, and indeed approaches bulk behavior very closely at high temperatures, for the thickest films. The same trend holds for both annealed films and for films with a rough surface layer. Another important trend emerges in the temperature variation $d\rho/dT$: Both sequences of films of

different thickness, those with a smooth and those with a rough surface layer, show that $d\rho/dT$ decreases systematically as the films become thinner. This behavior is contrary to the simple predictions of all common theories of such effects. These theories lead to a $d\rho/dT$ of thin films almost invariably larger than in bulk (for $K \lesssim 1$) and increasing for smaller K either because t decreases or λ becomes larger as the temperature is lowered.¹⁰

Values of $d\rho/dT$ less than in bulk have been

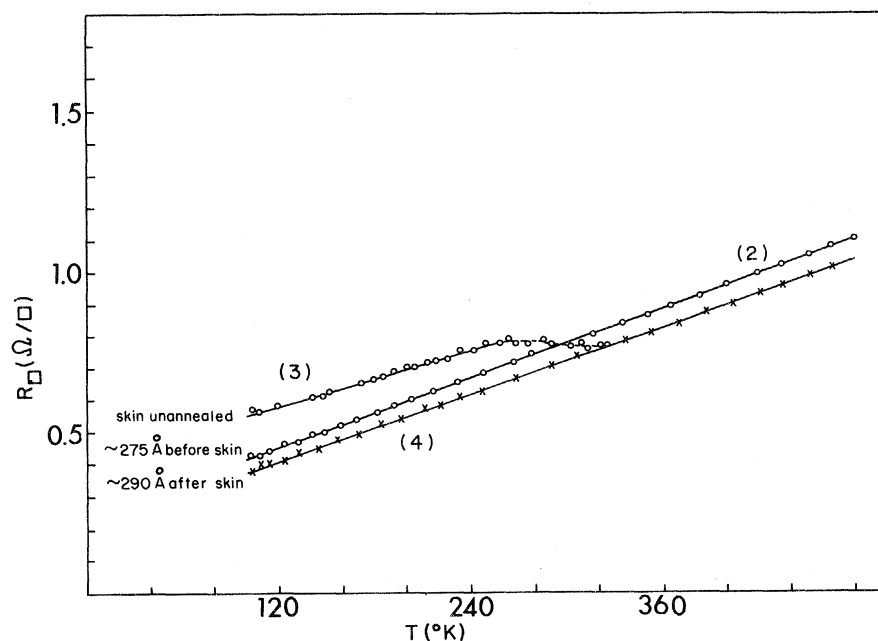


FIG. 3. Film resistance vs T for steps (2)-(4) of the experimental sequence.

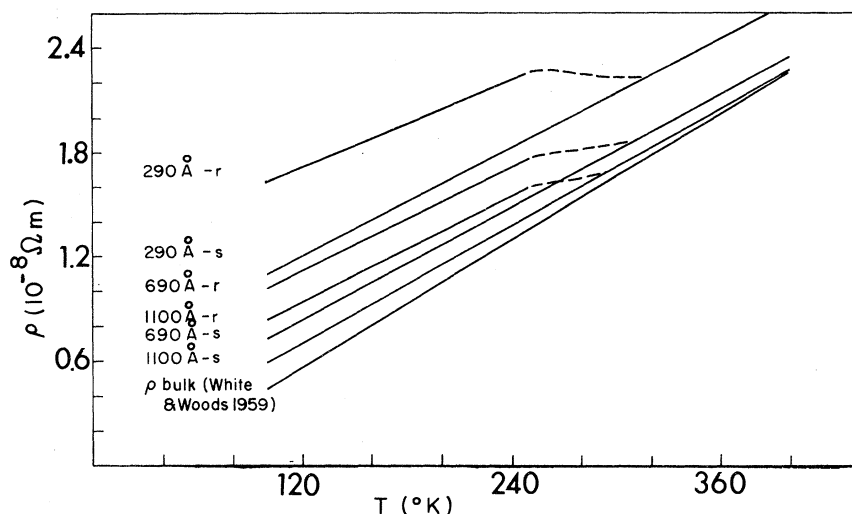


FIG. 4. Resistivities of three silver layers with a rough surface (*r*), and after annealing (*s*), as a function of temperature. Bulk data are also included.

found in most measurements in thin films. Generally either no use is made of this information in attempting an interpretation in terms of a theory (although the theory is invoked to explain the values of α), or the data are ascribed to effects of altered "bulk" behavior in the thin films under study, such as perhaps resulting from the existence of pores within the film, or from additional scattering by high and temperature-dependent strains introduced by the method of preparation of the films. The results presented here argue for a true size effect. First, while pores in the thinner films cannot be completely ruled out, the same behavior occurs in the fully continuous thicker films whose high-temperature values of ρ agree well with bulk. Furthermore, the strain dependence of the resistivity of these films is too small by a large factor to contribute to the observed decrease in $d\rho/dT$ as a consequence of differential thermal expansion of substrate and film material.¹¹ Finally, the lowering of $d\rho/dT$ persists if only the properties of the outermost surface layer are altered and nothing is changed in the bulk properties of the films. We must conclude that whenever the potential role of size effects is increased, such as by going to thinner films, or by producing a rougher surface, $d\rho/dT$ decreases. (Why $d\rho/dT$ is constant over the whole range of temperatures of our measurement is not fully clear since lower temperatures should also move the sample further into the size-effect regime. Perhaps the range of T is not sufficiently large, or perhaps other phenomena obscure any variation of $d\rho/dT$ with T .)

Thus an explanation of our data in terms of a size-effect theory must account quantitatively for: (a) increases of ρ and decreases of $d\rho/dT$ with decreasing film thickness, (b) increases of ρ and de-

creases of $d\rho/dT$ with increasing surface roughness, and (c) constancy of $d\rho/dT$ with T for a given film. Furthermore, it must include the fact that (d) the silver-mica interface has constant properties throughout the whole sequence of layers in Fig. 4, and (e) the bulk properties of all annealed layers are probably the same. The properties of the other surface, either when rough or when annealed, may vary from film to film and must come out of the experimental data.

IV. DATA ANALYSIS

All discussion of size effects relies on comparing the resistivity in thin samples to that of bulk material. Accurate knowledge of the bulk resistivity ρ_{bulk} is necessary and becomes particularly important when the deviations from bulk are very small, as in our thick films at elevated temperatures. Detailed data for ρ_{bulk} of silver in the range 100–300 °K are not extensive, and they do not fully agree with each other.¹² We have chosen for comparison the data of White and Woods giving ρ_{bulk} in ten-degree intervals in this temperature range. Figure 4 indicates that the bulk resistivity of infinitely thick samples prepared in the manner of our films cannot differ from that of bulk silver by a temperature-independent contribution caused by static imperfections or pores, since at high temperatures the thick films and bulk silver have common resistivities. This does not rule out a temperature-dependent correction to ρ_{bulk} that becomes important at lower temperatures. As an example of the effect of such correction, we include among our analyses below one using a ρ_{bulk} modified by strain of the differential thermal expansions of film and substrate.

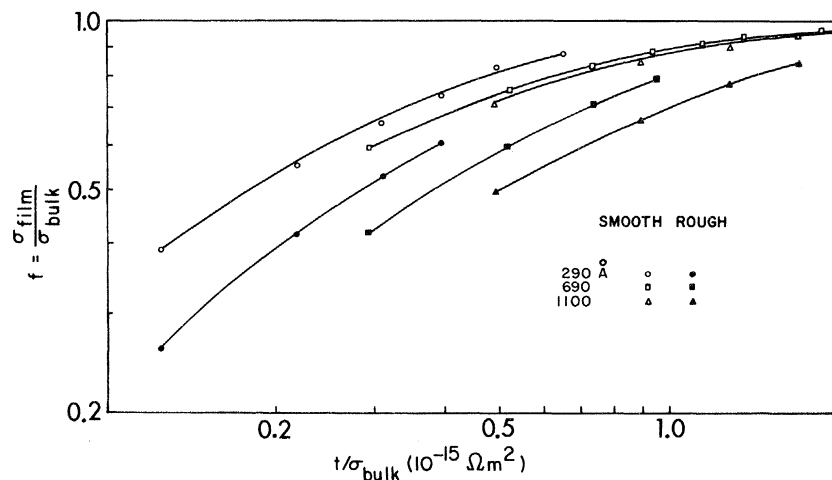


FIG. 5. Reduced form of data of Fig. 4. Lines connect points of given thickness, for two surface conditions.

To relate the data of Fig. 4 directly to size-effect theory we recast them into normalized form by using as ordinate the relative conductivity

$$f = \sigma_{\text{film}} / \sigma_{\text{bulk}}, \quad (1)$$

and as abscissa the ratio t/σ_{bulk} that differs from the parameter K by a constant factor. On a logarithmic scale this unknown factor does not distort the information, and it can easily be determined by the horizontal shift needed for match of experiment and theory. The reduced data are shown in Fig. 5. They confirm the conclusion of Sec. III that the simplest size-effect theory, which predicts a universal curve for *fixed surface conditions*, does not apply to either of the two film families, with smooth or rough outer surface. On the other hand, if all films in each family have common surface properties that change with temperature, we expect that the data for all thick-

nesses at a given temperature lie on the universal curve for some particular surface conditions.

Figure 6 represents the data of Fig. 4 according to this scheme. Compared to Fig. 5 this new grouping emphasizes two features. First there is more of an indication of universal behavior, especially among the films with smooth surfaces. Second, each isotherm varies more slowly with K , more in line with expectations of size-effect theory.

To make this comparison quantitative we must employ a formulation of size-effect theory that treats the two film surfaces separately. For the Fuchs-Sondheimer model,¹³ in which the surface scattering is represented by a specular parameter p , and where the conventional formulation is given by

$$f = \Phi(K; p), \quad (2)$$

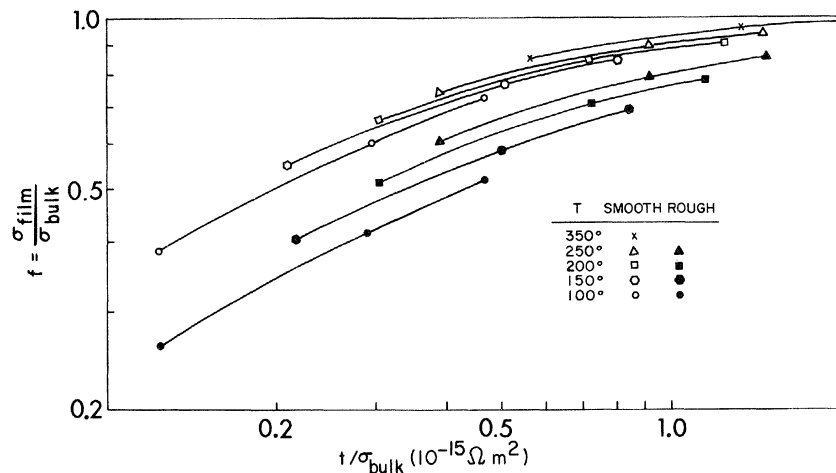


FIG. 6. Reduced form of data of Fig. 4. Lines connect points of common temperature, for two surface conditions.

the generalization to two surfaces with specularity parameters P and Q takes the form^{14,15}

$$f = \frac{(1-P)(1-Q)}{[1-(PQ)^{1/2}]^2} \Phi(K; (PQ)^{1/2}) + \left(1 - \frac{(1-P)(1-Q)}{[1-(PQ)^{1/2}]^2} \right) \Phi(2K; PQ) . \quad (3)$$

Equation (3) results in predictions like those of Fig. 7, which closely resemble the experimental curves of Fig. 6. In fact, the three lines in Fig. 6 referring to films with rough surfaces at 150, 200, and 250 °K superimpose perfectly on the lines of Fig. 7 by matching the horizontal scales such that $K=1$ corresponds to $t/\sigma_{\text{bulk}} = 0.85 \times 10^{-15} \Omega \text{m}^2$. The three lines belong to the parameter pairs $(P, Q) = (0, 0.2)$, $(0, 0.4)$, and $(0, 0.6)$. The line at 100 °K falls on the $(0, 0)$ line of Fig. 7 by a somewhat smaller shift ($K=1$ corresponds to $0.90 \times 10^{-15} \Omega \text{m}^2$), perhaps because of inaccuracies in the data, or because at low temperatures the relation between λ and σ_{bulk} is changing.

Evidently, the common parameter $P=0$ of all four curves refers to the rough film surface produced by the skin, so that $P_r=0$, and therefore Q describes the specularity of the silver-mica interface at different temperatures. With Q thus known, and the K scales established, the specularity parameter P_s of each smooth surface can be read off by superimposing the experimental f curves for the annealed films of Fig. 6 on a family of theoretical graphs of f similar to Fig. 7 of the given Q and the full range of P . The results of this procedure are summarized in Table I for all six films at five different temperatures. It shows that there exists a solution for all films within the allowed range of P_s and the common values of Q ,

TABLE I. Size-effect parameters of the data of Fig. 4, using the Fuchs-Sondheimer model of Eq. (3).

T (°K)	100	150	200	250	300
P_r	0.0	0.0	0.0	0.0	0.0
Q	0.0	0.2	0.4	0.6	0.9
$K(290 \text{ \AA})$	0.14	0.26	0.37	0.47	0.57
$P_s(290 \text{ \AA})$	1.0	0.8	0.7	0.6	0.5
$K(690 \text{ \AA})$	0.34	0.62	0.86	1.13	1.35
$P_s(690 \text{ \AA})$	1.0	0.9	0.8	0.7	0.6
$K(1100 \text{ \AA})$	0.53	0.99	1.38	1.78	2.15
$P_s(1100 \text{ \AA})$	1.0	1.0	0.9	0.9	0.8
$\lambda_{\text{bulk}} (\text{\AA})$	2100	1100	780	620	510

a fact which is not self-evident from the search procedure. Furthermore, since it spans the full range of the physically meaningful values of P_s and Q , the solution prescribed in Table I is quite unique (within the one significant figure assigned to the specularity parameters) and, in particular, there is practically no arbitrariness in the choice of the K scale. The table also lists the bulk mean free path at five temperatures. Discussion of the physical significance of this solution is postponed until after presentation of the analysis according to other size-effect models.

In the size-effect theory of Parrott,¹⁶ and Brandli and Cotti,¹⁷ where collisions with the surface are either totally diffuse or totally specular, depending on the angle of incidence, the parameter to be determined is the angle θ dividing the two domains. If for a common angle of both surfaces, the theory takes the form

$$f = \Psi(K; \theta) , \quad (4)$$

then the generalization to two surfaces of differing θ is¹⁸ for $\theta_2 > \theta_1$, as measured from the surface

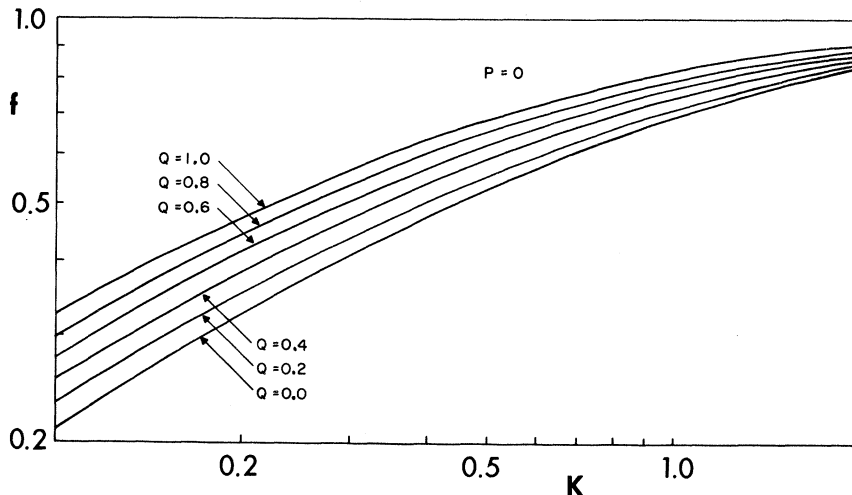


FIG. 7. Size-effect predictions of the generalized Fuchs-Sondheimer model of Eq. (3), for $P=0$, and various values of Q .

TABLE II. Size-effect parameters of the data of Fig. 4, using the θ cutoff model of Eq. (5).

T (°K)	100	150	200	250	300
θ_r (deg)	90	90	90	90	90
θ_Q (deg)	90	85	75	70	60
K (290 Å)	0.14	0.29	0.41	0.53	0.64
θ_s (290 Å) (deg)	0	0	45	50	55
K (690 Å)	0.34	0.70	0.96	1.30	1.55
θ_s (690 Å) (deg)	0	0	0	0	0
K (1100 Å)	0.53	1.12	1.55	2.00	2.40
θ_s (1100 Å) (deg)	0	0	0	0	0
λ_{bulk} (Å)	2100	980	710	550	460

normal,

$$f = \Psi(K; \theta_1) + \Psi(2K; \theta_2) - \Psi(2K; \theta_1). \quad (5)$$

A family of curves of f describing essentially the same situation as Fig. 6, is shown in Fig. 8. A parameter search following the procedure already outlined leads to the solution given in Table II, where the notation r , s designating the state of the outer surface, and Q labeling the silver-mica interface used in Table I, is continued. Just as in the previous analysis the solution is fairly unique, and spans the full range of θ . The surface properties follow the same pattern as before, and the K scale leads to comparable values of the bulk mean free path.

As a test of the sensitivity of the interpretation of size effects to the theoretical model, we have analyzed the data of Fig. 4 using a third model that incorporates the anisotropy of the Fermi surface of silver. In bulk the two major portions of this surface, belly and necks, have associated conductivities $\sigma_{\text{bulk}}^{(b)}$ and $\sigma_{\text{bulk}}^{(n)}$ that show different variation with temperature.¹⁹ Below room temperature $\sigma_{\text{bulk}}^{(n)}$ varies with T much more slowly than $\sigma_{\text{bulk}}^{(b)}$. In thin films with a (111) surface normal the two conductivities are expected to be affected differently by surface scattering, since some of the neck

TABLE IV. Size-effect parameters of the data of Fig. 4, using the model of Eq. (3), but with the *initial* thickness of the rough surface film.

T (°K)	100	150	200	250	300
P_r	0.0	0.0	0.0	0.0	0.0
Q	0.0	0.2	0.5	0.8	1.0
K (275 Å)	0.15	0.26	0.38	0.46	0.59
P_s (275 Å)	0.9	0.8	0.7	0.5	0.4
K (670 Å)	0.36	0.64	0.91	1.14	1.27
P_s (670 Å)	0.9	0.8	0.7	0.5	0.4
K (1075 Å)	0.59	1.02	1.42	1.85	2.30
P_s (1075 Å)	0.9	0.8	0.7	0.5	0.4
λ_{bulk} (Å)	1800	1100	740	590	470

carriers travel mostly parallel to the film surface, while the belly electrons have isotropic momenta. Based on this description, we assume that the film conductivity is given by

$$\sigma_{\text{film}} = f_b \sigma_{\text{bulk}}^{(b)} + \sigma_{\text{bulk}}^{(n)}. \quad (6)$$

To limit the number of variables we further assume that $\sigma_{\text{bulk}}^{(n)}$ is a temperature-independent constant determined from the experiment, and that the surface scattering of the belly electrons is also temperature independent. A proper solution requires that for the chosen value of $\sigma_{\text{bulk}}^{(n)}$ all smooth films fall on one universal curve, while all rough films fall on another (though the conversion to the K scale may be a function of temperature). Such a solution is listed in Table III, where the belly electrons are treated according to Fuchs-Sondheimer theory. It is interesting to note that in this solution the observed small values of $d\rho/dT$ are ascribed entirely to the shift in relative contributions of $\sigma_{\text{bulk}}^{(n)}$ and $\sigma_{\text{bulk}}^{(b)}$ to σ_{bulk} at different temperatures. The mean free path of the dominant carriers is comparable to that in the other models.

Two additional analyses of the data of Fig. 4 are presented. In the first, summarized in Table IV, it is assumed that the thickness of the film with a

TABLE III. Size-effect parameters of the data of Fig. 4 using a two-band bulk conductivity $\sigma_{\text{bulk}} = \sigma_{\text{bulk}}^{(n)} + \sigma_{\text{bulk}}^{(b)}$, with the belly conductivity obeying the Fuchs-Sondheimer model, Eq. (6).

T (°K)	100	150	200	250	300
$\sigma_{\text{bulk}}^{(n)}$ ($10^8/\Omega m$)	0.08	0.08	0.08	0.08	0.08
$\sigma_{\text{bulk}}^{(b)}$ ($10^8/\Omega m$)	2.21	1.26	0.872	0.660	0.525
$P_r^{(b)}$	0.0	0.0	0.0	0.0	0.0
$Q^{(b)}$	0.0	0.0	0.0	0.0	0.0
$P_s^{(b)}$	1.0	1.0	1.0	1.0	1.0
$K^{(b)}$ (290 Å)	0.15	0.26	0.38	0.51	0.64
$K^{(b)}$ (690 Å)	0.35	0.63	0.90	1.19	1.53
$K^{(b)}$ (1100 Å)	0.56	1.02	1.46	1.93	2.43
$\lambda_{\text{bulk}}^{(b)}$ (Å)	2000	1100	770	580	450

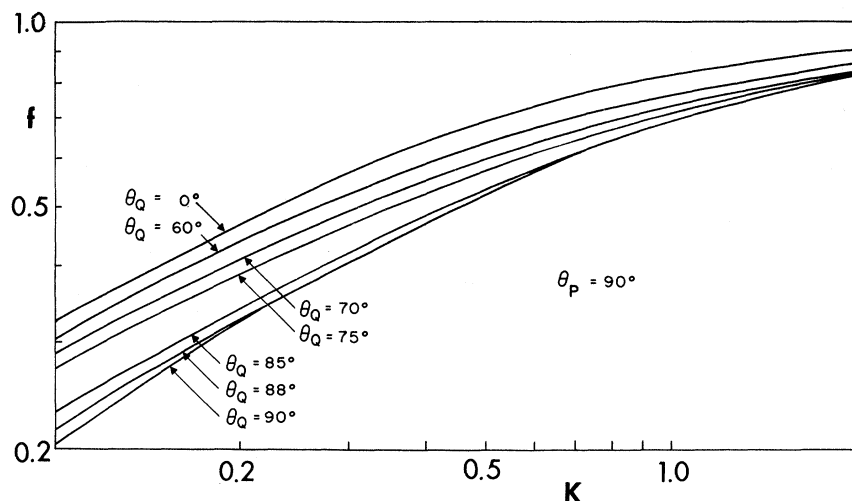


FIG. 8. Size-effect predictions of the generalized θ -cutoff model of Eq. (5), for $\theta_P = 90^\circ$, and various values of θ_Q .

rough surface skin is that prior to the deposition of the skin, a supposition suggested by the observation that the increase in film resistance with rough skin is independent of the skin thickness between about 10 and 50 Å. The solution is very similar to that of Table I, except that the K scales are shifted slightly. In the last analysis we assume that the proper bulk conductivity is reduced because of thermal strain existing in the film at all temperatures below the deposition temperature. Using data on the strain dependence of resistivity of films prepared in the same manner,¹¹ the corrected bulk properties lead to a new set of reduced variables. The analyses of these data result in the parameters of the Fuchs-Sondheimer model given in Table V. Except for minor shifts in scale, they fully repeat the trends of Table I.

V. CONCLUSIONS

We have shown that a systematic experiment can produce raw data that are sufficiently complete and independent to justify their critical analysis of terms of size-effect theory. By preserving one

common interface for six films, and by strongly modifying the properties of the second film surface, leaving the other film properties untouched, the experiment removes many of the uncertainties of most thin-film data. At the same time, these interconnections put much more stringent conditions than usual on the match with theory.

As a result it is not at all self-evident that the data can be fitted to any one theory. It is a measure of the similarity of the predictions of the various theories that we have been able to find a solution in every case examined. Each such solution is quite unique and leads to reasonable parameters; it also requires going somewhat beyond the traditional formulations of size-effect theory. Perturbations in the data such as introduced in Tables IV and V lead to similar and neighboring solutions, indicating that the conclusions are not crucially dependent on the exact input data.

The outstanding characteristic of the isotropic models is the temperature dependence of the specularly parameters at the mica-silver interface and at the free smooth surface. In contrast, the

TABLE V. Size-effect parameters of the data of Fig. 4, using the model of Eq. (3) with a reference bulk conductivity modified by thermal differential strain.

T (°K)	100	150	200	250	300
σ_{bulk} ($10^8/\Omega m$)	1.74	1.16	0.870	0.695	0.582
P_r	0.0	0.0	0.0	0.0	0.0
Q	0.5	0.7	0.8	0.9	1.0
K (290 Å)	0.14	0.22	0.31	0.38	0.48
P_s (290 Å)	0.6	0.6	0.5	0.5	0.5
K (690 Å)	0.34	0.52	0.72	0.90	1.08
P_s (690 Å)	0.8	0.8	0.7	0.7	0.7
K (1100 Å)	0.54	0.84	1.14	1.45	1.75
P_s (1100 Å)	1.0	0.9	0.9	0.8	0.8
λ_{bulk} (Å)	2000	1300	960	760	630

anisotropic model explains the abnormal behavior of dp/dT by the differing influence of the surface on neck and belly electrons, and leaves all surface specular parameters independent of temperature.

On the basis of the analysis given here it is not possible to choose between the various theories, or to conclude that the temperature variation of surface scattering found in some models is real. Before more definite conclusions can be reached, it is essential that any analysis includes a stricter knowledge of bulk properties, including the distribution of carrier properties over the Fermi sur-

face, and of the modifications of those bulk properties introduced by the method of preparation of the thin films. At that point a more realistic theory of size effects is probably also in order.

The size-effect parameters we have deduced from the resistance data allow us to predict absolutely other size-dependent transport phenomena. We have applied this information to study the origin of the metallic field effect.⁴ More generally, an examination of more than one transport property is probably essential before a particular theory of size effects, and its conditions, can be singled out.

*Supported in part by the Joint Services Electronics Program, the Office of Naval Research, and the National Science Foundation.

[†]Present address: Dept. of Phys., New York City Community College, Brooklyn, N. Y. 11201.

¹J. M. Ziman, *Electrons and Phonons* (Oxford U. P., Oxford, England, 1960), Chap. 11.

²K. L. Chopra, *Thin Film Phenomena* (McGraw-Hill, New York, 1969), Chap. 6.

³A. Berman, Ph.D. thesis (Polytechnic Institute of Brooklyn, 1970) (unpublished). Preliminary accounts of this work have been given in *Bull. Am. Phys. Soc.* **16**, 144 (1971); and in *Appl. Phys. Lett.* **18**, 415 (1971).

⁴A. Berman and H. J. Juretschke, following paper, *Phys. Rev. B* **11**, 2903 (1975).

⁵L. Goldstein and B. Post, *J. Appl. Phys.* **40**, 3056 (1969).

⁶D. W. Pashley and M. J. Stowell, *Philos. Mag.* **8**, 1605 (1963).

⁷M. S. P. Lucas, *Appl. Phys. Lett.* **4**, 73 (1964).

⁸K. L. Chopra and M. R. Randlett, *J. Appl. Phys.* **38**, 144 (1967).

⁹G. K. White and S. B. Woods, *Philos. Trans. R. Soc. Lond. A* **251**, 273 (1959).

¹⁰D. S. Campbell, in *Use of Thin Films in Physical Investigations*, edited by J. C. Anderson (Academic, New York, 1966), p. 314.

¹¹B. S. Verma and H. J. Juretschke, *J. Appl. Phys.* **41**, 4732 (1970).

¹²L. A. Hall, *Natl. Bur. Stand. (U. S.) Tech. Note* 365 (U. S. GPO, Washington, D. C., 1968).

¹³E. Sondheimer, *Adv. Phys.* **1**, 1 (1952).

¹⁴H. J. Juretschke, *Surf. Sci.* **2**, 40 (1964).

¹⁵M. S. P. Lucas, *J. Appl. Phys.* **36**, 1632 (1965).

¹⁶J. E. Parrott, *Proc. Phys. Soc. Lond.* **85**, 1143 (1965).

¹⁷G. Brandli and P. Cotti, *Helv. Phys. Acta* **38**, 801 (1965).

¹⁸H. J. Juretschke, *Surf. Sci.* **5**, 111 (1966).

¹⁹J. M. Ziman, *Phys. Rev.* **121**, 1320 (1961).